Palladium Cluster Compounds

$[Pd_{30}(CO)_{26}(PEt_3)_{10}]$ and $[Pd_{54}(CO)_{40}(PEt_3)_{14}]$: Generation of Nanosized Pd_{30}- and Pd_{54}-Core Geometries Containing Interpenetrating Cuboctahedral-Based Metal Polyhedra**

*Eugeny G. Mednikov, Sergei A. Ivanov, and Lawrence F. Dahl**

Herein, we report the synthesis and structural features of the two new palladium carbonyl phosphane clusters $[Pd_{30}(\mu_2\text{-}CO)_{22}(\mu_3\text{-}CO)_4(PEt_3)_{10}]$ (**1**) and $[Pd_{54}(\mu_2\text{-}CO)_{32}(\mu_3\text{-}CO)_8(PEt_3)_{14}]$ (**2**). Their nanosized Pd_{30} and Pd_{54} cores are the first examples of so-called "twinned"-core geometries involving a previously unknown oligomeric growth pattern, comprised of interpenetrating cuboctahedra as building blocks (that is, corresponding to selective ccp/hcp layer stacking; ccp = cubic close-packed, hcp = hexagonal close-packed). These results have particular stereochemical implications concerning multi-twinned structures[1] and growth sequences of much larger ligated and nonligated palladium nanoparticles.[2–6] The previously unknown cuboctahedral-twinned palladium-core geometries in **1** and **2** provide additional stereochemical evidence that emphasizes the highly versatile nature of this unique transition metal in readily forming a remarkable array of highly condensed carbonyl–phosphane clusters with either icosahedral-, ccp-, or mixed ccp/hcp-based metal-core arrangements.[4d,7–11] Palladium clusters also have considerable general interest since palladium has special commercial importance in that it forms exceptionally efficient mono- and bimetallic catalysts for organic transformations.

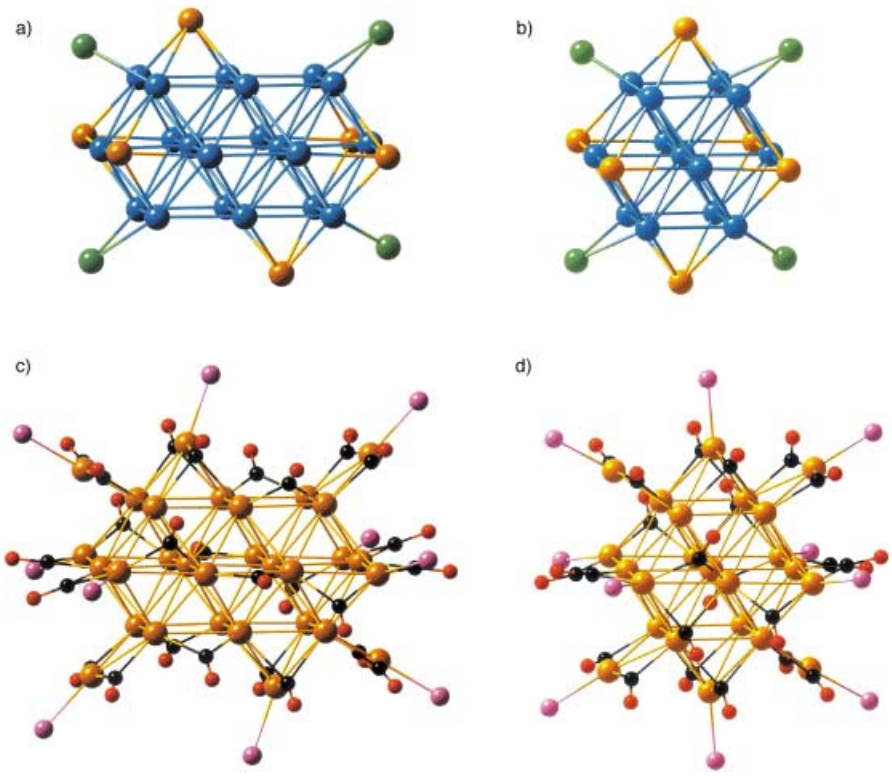

Figure 1. a) Pd_{30} pseudo-C_{2h} (2/m) core geometry in $[Pd_{30}(CO)_{26}(PEt_3)_{10}]$ (**1**). The maximum metal-core diameter (excluding the wingtip Pd atoms) between two symmetry-equivalent pairs of centrosymmetrically opposite (square-face)-capping Pd atoms (orange) is 1.01 nm; inclusion of the wingtip Pd atoms results in two symmetry-equivalent pairs of centrosymmetrically related wingtip atoms with metal-core diameters of 1.14 nm; b) Pd_{23}-core geometry in the known $[Pd_{23}(CO)_{20}(PEt_3)_{10}]$ (**3**).[10,11] The centered Pd_{13} kernel (blue) corresponds to a standard ccp arrangement about a centered atom; c) Structure of **1** which shows ten terminal PEt_3 ligands (without ethyl substituents for clarity) and 26 bridging CO groups about the Pd_{30} core. Pseudo-C_{2h} symmetry is maintained with the C_2 axis passing through two bridging CO groups and with the σ_h mirror plane (approximately coinciding with the paper) containing four bicuboctahedral Pd atoms, as well as two (square-face)-capping Pd atoms and four wingtip Pd atoms, together with their six attached phosphane P atoms. The two tetracapping $\{Pd(PEt_3)\}$ fragments lying on the mirror plane are each connected by two μ_3-CO groups to four basal Pd atoms in shell 1, while the other four tetracapping and four wingtip $\{Pd(PEt_3)\}$ fragments in shell 2 are each linked by 2 μ_2-CO groups to 14 Pd atoms in shell 1. The remaining six μ_2-CO groups are linked to three adjacent pairs of centrosymmetrically opposite bicuboctahedral Pd atoms in shell 1; d) Structure of **3** showing the analogous distribution of 10 terminal PEt_3 ligands (without ethyl substituents) and 20 bridging CO groups about the Pd_{23} core.[10,11]

Crystals of both **1** and **2** were reproducibly obtained as by-products together with $[Pd_{38}(CO)_{28}(PEt_3)_{12}]$[8h,i,12] through the deligation of $[Pd_{10}(CO)_{12}(PEt_3)_6]$ [8a,9a] with CO assistance at the initial stage of the reaction.[13,14] The molecular geometries and stoichiometries of **1** and **2** were unambiguously established from X-ray crystallographic analysis.[15]

The pseudo-C_{2h} (2/m) geometry of the Pd_{30} core of $[Pd_{30}(CO)_{26}(PEt_3)_{10}]$ (**1**; Figure 1 a) is composed of two interpenetrating centered Pd_{13} cuboctahedra (blue), which form a "twinned" centered Pd_{20} bicuboctahedron (blue, with six common atoms) that is capped on six of its eight square faces by six Pd atoms (orange) and additionally edge-bridged by four exopolyhedral wingtip Pd atoms (green). The crystallographically required centrosymmetric Pd_{30} geometry of **1** (Figure 1 a) is closely related to the Pd_{23} geometry (Figure 1 b) of the known $[Pd_{23}(CO)_{20}(PEt_3)_{10}]$ cluster (**3**), which is composed of a centered Pd_{13} cuboctahedron (blue) with six

[*] Prof. L. F. Dahl, Dr. E. G. Mednikov, Dr. S. A. Ivanov
Department of Chemistry
University of Wisconsin-Madison
1101 University Avenue, Madison, WI 53706 (USA)
Fax: (+1) 608-262-6143
E-mail: dahl@chem.wisc.edu

[**] This research was supported by the National Science Foundation (CHE-9729555). The CCD area detector system was purchased, in part, with a NSF grant (CHE-9310428). Color figures were prepared with Crystal Maker, Interactive Crystallography (version 5; David C. Palmer, P.O. Box 183, Bicester, Oxfordshire, OX26 3TA (UK)). We are indebted to Dr. Ilia Guzei (UW-Madison) for helpful crystallographic advice.

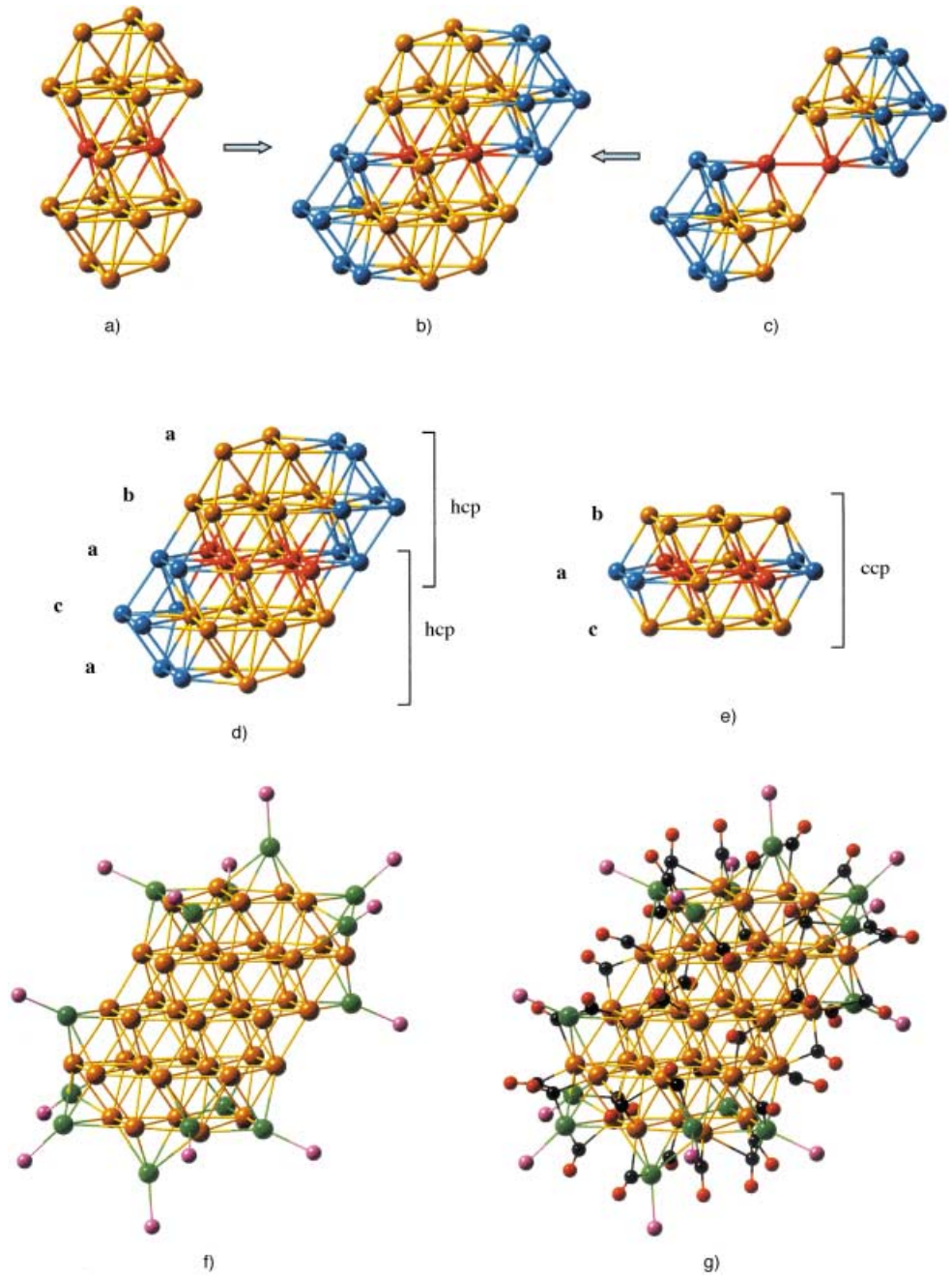

Figure 2. a) Central Pd_{38} fragment of the Pd_{54} core in C_i $[Pd_{54}(CO)_{40}(PEt_3)_{14}]$ (**2**), composed of four interpenetrating centered anti-cuboctahedra (hcp) generated by superposition of Pd_{24} fragment (left) and Pd_{26} fragment (right); b) Pd_{24} fragment consisting of two interpenetrating centered anti-cuboctahedra with a common Pd–Pd edge; c) Pd_{26} fragment consisting of two connected but non-interpenetrating centered anti-cuboctahedra. d) Pd_{40} fragment of the Pd_{54} core consists of a five-layer mixed hcp/ccp stacking arrangement formed from the central Pd_{38} fragment and two centrosymmetrically related Pd atoms (red) to the middle (equatorial) layer. The resulting 40-atom framework has a close-packed (**a**(Pd_5) **b**(Pd_{10}) **a**(Pd_{10}) **c**(Pd_{10}) **a**(Pd_5)) sequence; the top and bottom three layers may be viewed as two interpenetrating 25-atom **aba** and **aca** hcp layers with a common middle layer; e) Pd_{20} fragment of three interior 30-atom layers, which has a **bac** ccp stacking arrangement that corresponds to two interpenetrating centered cuboctahedra with six common atoms and completely coincides with Pd_{20} core of cluster **1**. f) Pd_{54}-core geometry obtained by the addition of 12 square-capping and two triangular-capping phosphane-attached Pd atoms (shell 2) to a Pd_{40} fragment composed of six interior coplanar Pd atoms forming four edge-fused equilateral triangles that are completely encapsulated by 34 Pd atoms (shell 1). Metal-core dimensions are $1.5 \times 1.2 \times 0.5$ nm; g) Structure of **2** displaying the arrangement of 14 PEt_3 ligands (without ethyl substituents) and 40 bridging CO groups about the Pd_{54} core.

  0044-8249/03/11503-0338 $ 20.00+.50/0

additional (square-face {100}) capping Pd atoms (orange) and four edge-bridging wingtip Pd atoms (green).[10,11] The 13 centered-cuboctahedral and six (square-face) capping Pd atoms in **3** may alternatively be viewed as a centered ν_2 Pd_{19} octahedron (that is, ν_n denotes $(n+1)$ equally spaced atoms along each edge) of pseudo-O_h (4/m$\bar{3}$2/m) symmetry with the other four wingtip Pd atoms lying on one of the octahedral mirror planes, such that the molecular symmetry is reduced to pseudo-D_{2h} (*mmm*). A geometrical comparison of the metal frameworks in **1** and **3** (Figure 1a, b) reveals that the pseudo-C_{2h} Pd_{30} core in **1** may be formally constructed from two of the centered Pd_{20} building-block-fragments in **3** (that is, the geometry of the Pd_{23} core, minus one face-capping and two wingtip Pd atoms) by a centrosymmetric interpenetration resulting in ten common atoms.

From a cluster shell model, both **1** and **3** may be regarded as possessing two and one interior Pd atoms, respectively, that are completely encapsulated in the first metal-coordination shell (shell 1) by 18 and 12 Pd atoms, respectively, that are not attached to PEt_3 groups; in turn, these first-shell Pd atoms are surrounded by ten bridging {$Pd(PEt_3)$} fragments in the second incomplete metal-coordination shell (shell 2) that are each connected to only the Pd atoms in shell 1. Figure 1c and d shows that a close geometrical resemblance exists between the entire ligated structures of **1** and **3**, with the CO and PEt_3 ligands in **1** occupying analogous coordination sites to those in **3**.[16,17]

The configuration of $[Pd_{54}(CO)_{40}(PEt_3)_{14}]$ (**2**) is given in Figure 2. Its close-packed "multi-twinned" Pd_{54}-core geometry of crystallographic $C_i(\bar{1})$ site-symmetry consists of a central five-layer Pd_{38} framework (Figure 2b) that may be formally considered as a fragment from a supracluster generated by the interpenetration of two anti-cuboctahedral Pd_{24} fragments (Figure 2a) and two anti-cuboctahedral Pd_{26} fragments (Figure 2c). These fragments each combine two anti-cuboctahedral (hcp) building blocks, with and without a common Pd–Pd edge, respectively. Addition of two centrosymmetrically related Pd atoms (red) to the middle (equatorial) layer of the Pd_{38} unit gives a Pd_{40} framework (Figure 2d) that is formed by the stacking of five layers in a mixed ccp/hcp (**a**(Pd_5) **b**(Pd_{10}) **a**(Pd_{10}) **c**(Pd_{10}) **a**(Pd_5)) sequence. This sequence reveals that the Pd_{40} framework can be regarded as the interpenetration of two centrosymmetrically equivalent 25-atom hcp three-layer **aba** and **aca** fragments, each containing a common middle layer (Figure 2d). 20 of the 30 Pd atoms in the inner three layers that have a **bac** ccp arrangement (Figure 2e) correspond to two interpenetrating centered Pd_{13} cuboctahedra (with six common Pd atoms). This Pd_{40} component of the Pd_{54}-core geometry of **2** may likewise be envisioned as a close-packed cluster shell-model with six interior Pd atoms conforming to a coplanar array of four edge-fused equilateral triangles that are completely surrounded by 34 Pd atoms (shell 1). Further condensation of 14 face-capping {$Pd(PEt_3)$} fragments gives rise to the incomplete second shell (Figure 2f). Figure 2g gives the configuration of **2** (without the phosphorus-attached ethyl substituents), which maintains crystallographic $C_i(\bar{1})$ symmetry. The entire Pd_{54} core is stabilized by 14 PEt_3 and 40 bridging carbonyl ligands.[16,17]

The identical geometrical conformity of the same central ccp Pd_{20} fragment in **1** (blue in Figure 1a) and **2** (Figure 2e) to a centered Pd_{20} bicuboctahedron, which formally arises through an interpenetrating "twinning" of the central cuboctahedral Pd_{13} fragment in **3** (blue in Figure 1b) suggests similar growth pathways. Prime evidence for this close architectural interrelationship of their cores is demonstrated by the fact that the mean Pd–Pd separations within the fragments are amazingly similar, in spite of the ellipsoidal Pd_{30}- and Pd_{54}-core geometries. Salient structural/bonding features and their resulting implications are: 1) Pd(i)–Pd(i) mean separations of 2.77 and 2.76 Å for the two and six interior Pd(i) atoms in the twinned cuboctahedral (ccp) and multi-twinned cuboctahedral (ccp/hcp)-based nanosized cores of **1** and **2**, respectively, which are analogous to the Pd–Pd separation of 2.75 Å found in ccp Pd metal.[18] This bond-length similarity is consistent with the interior palladium atoms being considered as having metallic character; 2) equivalent radial Pd(i)–Pd(s_1) and tangential Pd(s_1)–Pd(s_1) mean separations of 2.82–2.84 Å for the first-shell Pd(s_1) atoms that completely surround the interior Pd(i) atoms in **1**, **2**, and **3**. Their essentially identical mean separations, which are expected for ccp/hcp cores in metal nanoparticles,[19] point to analogous charge distributions for the similarly coordinated Pd(s_1) atoms, without undue strain effects being sterically imposed by the elliptical "twinned" cuboctahedral-based cores of **1** and **2**. The fact that the mean separations are approximately 0.08 Å longer than that of the interior Pd(i)–Pd(i) interactions can be attributed to ligation influences of the CO and $Pd(PEt_3)$ bridging units; 3) shorter mean Pd(s_1)–Pd(s_2) separations (by 0.024–0.062 Å), relative to the corresponding Pd(s_1)–Pd(s_1) interactions, can be readily ascribed to the bond-shortening influence of the two bridging CO groups that connect each capping {$Pd(PEt_3)$} unit (denoted as Pd(s_2)) to the Pd(s_1) atoms; and 4) their virtually identical overall mean Pd–Pd bonding connectivities of 2.81 Å which likewise signify that similar types of core geometries in palladium–carbonyl–phosphane clusters strongly influence its resulting metal–metal bonding characteristics.

A major outcome of this research is that the unprecedented metal-core architectures of **1** and **2** represent a hitherto unknown type of oligomerization as interpenetrating twinned composites of cuboctahedral (ccp/hcp) building blocks. The fact that **1** and **2** are by-products of the same reaction suggests a similar growth pattern that had not been previously encountered.

Received: October 14, 2002 [Z50363]

[1] L. D. Marks, *Rep. Prog. Phys.* **1994**, *57*, 603, and references therein.

[2] a) J. S. Bradley, E. W. Hill, S. Behal, C. Klein, B. Chaudret, A. Duteil, *Chem. Mater.* **1992**, *4*, 1234; b) C. Amiens, D. de Carlo, B. Chaudret, J. S. Bradley, R. Mazel, C. Roucau, *J. Am. Chem. Soc.* **1993**, *115*, 11638; c) M. J. Yacaman, J. A. Ascencio, H. B. Liu, J. Gardea-Torresdey, *J. Vac. Sci. Technol.* **2001**, *B19*, 1091; d) H. Bönnemann, R. M. Richards, *Eur. J. Inorg. Chem.* **2001**, 2455;

e) N. Toshima, T. Yonezawa, *New J. Chem.* **1998**, *2*, 1179, and references therein.

[3] Noncrystalline N,O-ligated (noncarbonyl) palladium nanoclusters possessing idealized formulations based upon concentric full-shell palladium cores have been reported: namely, five-shell Pd_{561} clusters[4,5] and mixtures of seven-shell Pd_{1415} and eight-shell Pd_{2057} clusters.[6]

[4] a) M. N. Vargaftik, V. P. Zagorodnikov, I. P. Stolyarov, I. I. Moiseev, V. A. Likholobov, D. I. Kochubey, A. L. Chuvilin, V. I. Zaikovsky, K. I. Zamaraev, G. I. Timofeeva, *J. Chem. Soc. Chem. Commun.* **1985**, 937; b) M. N. Vargaftik, I. I. Moiseev, D. I. Kochubey, K. I. Zamaraev, *Faraday Discuss.* **1991**, *92*, 13; c) "Catalysis with Palladium Clusters": I. I. Moiseev, M. N. Vargaftik in *Catalysis by Di- and Polynuclear Metal Cluster Compounds* (Eds.: R. D. Adams, F. A. Cotton), Wiley-VCH, New York, **1998**, p. 395; d) T. A. Stromnova, I. I. Moiseev, *Russ. Chem. Rev.* **1998**, *67*, 485.

[5] a) G. Schmid, *Polyhedron* **1988**, *7*, 2321; b) G. Schmid, *Chem. Rev.* **1992**, *92*, 1709.

[6] G. Schmid, M. Harms, J.-O. Malm, J.-O. Bovin, J. van Ruitenbeck, H. W. Zandbergen, W. T. Fu, *J. Am. Chem. Soc.* **1993**, *115*, 2046.

[7] a) N. K. Eremenko, E. G. Mednikov, S. S. Kurasov, *Russ. Chem. Rev.* **1985**, *54*, 394, and references therein; b) N. K. Eremenko, S. P. Gubin, *Pure Appl. Chem.* **1990**, *62*, 1179; c) A. D. Burrows, D. M. P. Mingos, *Transition Met. Chem.* **1993**, *18*, 129, and references therein; d) R. B. King, *Gazz. Chim. Ital.* **1992**, *122*, 383; e) K. R. Dixon, A. C. Dixon, *Comprehensive Organometallic Chemistry II, Vol. 9* (Eds.: E. W. Abel, F. G. A. Stone, G. Wilkinson, R. J. Puddephatt), Elsevier, Tarrytown, NY, **1995**, p. 194; f) T. A. Stromnova, I. I. Moiseev, *Russ. Chem. Rev.* **1998**, *67*, 485, and references therein; g) E. G. Mednikov, S. A. Ivanov, I. A. Guzei, L. F. Dahl, *Abst. of Papers*, 222nd ACS National Meeting of American Chemical Society, Chicago, IL.; American Chemical Society, Washington, DC, **2001**, INORG 331.

[8] a) $[Pd_{10}(CO)_{12}(PR_3)_6]$ (R = *n*Bu, Et): E. G. Mednikov, N. K. Eremenko, *Izv. Akad. Nauk SSSR Ser. Khim.* **1982**, 2540. [E. G. Mednikov, N. K. Eremenko, *Russ. Chem. Bull.* **1983**, *32*, 2240 (*Engl. Trans.*)]; b) $[Pd_{10}(CO)_{14}(PnBu_3)_4]$: E. G. Mednikov, N. K. Eremenko, Yu. L. Slovokhotov, Yu. T. Struchkov, S. P. Gubin, *J. Organomet. Chem.* **1983**, *258*, 247; c) $[Pd_{10}(CO)_{12}(PPh_3)_6]$: E. G. Mednikov, N. K. Eremenko, *Izv. Akad. Nauk SSSR Ser. Khim.* **1984**, 2781. [E. G. Mednikov, N. K. Eremenko, *Russ. Chem. Bull.* **1984**, *33*, 2547 (*Engl. Trans.*)]; d) $[Pd_{12}(CO)_{12}(PnBu_3)_6]$: E. G. Mednikov, Yu. T. Struchkov, Yu. L. Slovokhotov, *J. Organomet. Chem.* **1998**, *566*, 15; e) $[Pd_{16}(CO)_{13}(PEt_3)_9]$: E. G. Mednikov, Yu. L. Slovokhotov, Yu. T. Struchkov, *Metalloorg. Khim.* **1991**, *4*, 123. [E. G. Mednikov, Yu. L. Slovokhotov, Yu. T. Struchkov, *Organomet. Chem. USSR* **1991**, *4*, 65 (*Engl. Trans.*)]; f) $[Pd_{23}(CO)_{20}(PEt_3)_8]$: E. G. Mednikov, N. K. Eremenko, Yu. L. Slovokhotov, Yu. T. Struchkov, *Zh. Vsesoyuzn. Khim. O-va im. D. I. Mendeleeva*, **1987**, *32*, 101 (*in Russian*); E. G. Mednikov, *Izv. Akad. Nauk SSSR Ser. Khim.* **1993**, 1299. [E. G. Mednikov, N. K. Eremenko, Yu. L. Slovokhotov, Yu. T. Struchkov, *Russ. Chem. Bull.* **1993**, *42*, 1242 (*Engl. Trans.*)]; g) $[Pd_{23}(CO)_{22}(PEt_3)_{10}]$: E. G. Mednikov, N. K. Eremenko, Yu. L. Slovokhotov, Yu. T. Struchkov, *J. Organomet. Chem.* **1986**, *301*, C35; E. G. Mednikov, *Metalloorg. Khim.* **1991**, *4*, 885. [E. G. Mednikov, *Organomet. Chem. USSR* **1991**, *4*, 433 (*Engl. Trans.*)]; h) $[Pd_{34}(CO)_{24}(PEt_3)_{12}]$, $[Pd_{38}(CO)_{28}(PR_3)_{12}]$, (R = Et, *n*Bu): E. G. Mednikov, N. I. Kanteeva, *Izv. Akad. Nauk SSSR Ser. Khim.* **1995**, 167 [E. G. Mednikov, N. I. Kanteeva, *Russ. Chem. Bull.* **1995**, *44*, 163 (*Engl. Trans.*)]; i) $[Pd_{38}(CO)_{28}(PEt_3)_{12}]$ (**5**): E. G. Mednikov, N. K. Eremenko, Yu. L. Slovokhotov, Yu. T. Struchkov, *J. Chem. Soc. Chem. Commun.* **1987**, 218; j) E. G. Mednikov, P. V. Petrovsky, Yu. L. Slovokhotov, O. A. Belyakova, N. I. Malkina, unpublished results; k) E. G. Mednikov, unpublished results.

[9] a) $[Pd_{10}(CO)_{12}(PEt_3)_6]$ (**4**): D. M. P. Mingos, C. M. Hill, *Croat. Chem. Acta* **1995**, *68*, 745; b) $[Pd_{145}(CO)_x(PEt_3)_{30}]$: N. T. Tran, D. R. Powell, L. F. Dahl, *Angew. Chem.* **2000**, *112*, 4287; *Angew. Chem. Int. Ed.* **2000**, *39*, 4121; c) $[Pd_{16}(CO)_{13}(PMe_3)_9]$, $[Pd_{35}(CO)_{23}(PMe_3)_{15}]$, $[Pd_{39}(CO)_{23}(PMe_3)_{16}]$, $[Pd_{59}(CO)_{32}(PMe_3)_{21}]$: N. T. Tran, M. Kawano, L. F. Dahl, *J. Chem. Soc. Dalton Trans.* **2001**, 2731.

[10] Interestingly, reactions of the $[Pd_{13}Ni_{13}(CO)_{34}]^{4-}$ tetraanion[11a] with PEt_3 produced, in addition to the known Pd_{10}, Pd_{16}, and Pd_{34} clusters,[8a,e,h] a different crystal form of $[Pd_{23}(CO)_{20}(PEt_3)_{10}]$[11b] that has the same Pd_{23} framework as that previously reported by Mednikov et al.[8g] for $[Pd_{23}(CO)_{22}(PEt_3)_{10}]$ but with two fewer CO groups; a comparative molecular analysis favors the existence of both clusters.[11b,c]

[11] a) N. T. Tran, M. Kawano, D. R. Powell, L. F. Dahl, *J. Chem. Soc. Dalton Trans.* **2000**, 4138; b) J. Wittayakun, N. T. Tran, D. R. Powell, L. F. Dahl, unpublished results; c) E. G. Mednikov, L. F. Dahl, unpublished results.

[12] In contrast to the generally close-packed metal frameworks of palladium carbonyl phosphanes, such as **1** and **2**, the metal-core geometry of $[Pd_{38}(CO)_{28}(PEt_3)_{12}]$ (**5**)[8i] cannot be described in terms of close-packing without invoking considerable distortions.

[13] In a typical procedure, $[Pd_{10}(CO)_{12}(PEt_3)_6]$ (**4**, 0.150 g, 0.071 mmol) was combined with a mixture of Me_2CO (7 mL), iPr_2O (2 mL), and CF_3CO_2H (0.1 mL) in a 100-mL flask and stirred at room temperature, initially under N_2 for 1 h, then under CO for 2 h, and finally under N_2. After two weeks, easily distinguishable black end-sharpened needle-shaped crystals of **1**·2 Me_2CO and black end-flattened needle-shaped crystals of **2**·2 Me_2CO were separated under the microscope from the black block-shaped crystals of $[Pd_{38}(CO)_{28}(PEt_3)_{12}]$ (**5**). Estimated yields of crystals of **1**·2 Me_2CO (less than 5%), **2**·2 Me_2CO (less than 1%), and **5**·2 Me_2CO (55–57%). Similar yields of crystals of **1** and **2** were obtained by direct treatment under CO (70–80 min) of solutions of **4** (0.150 g) in Me_2CO (7 mL), Et_2O (2 mL), HOAc (0.17 mL), and CF_3CO_2H (0.05 mL) followed by crystallization under N_2. Compound **2** was also prepared as a minor product without the assistance of CO but in the presence of HCO_2H instead of HOAc, and either with or without CF_3CO_2H.[14] None of the reactions without CO have given **1**. IR spectra of **1** and **2** (Nujol, CaF_2 cell) exhibited bridging CO groups at 1910 (m), 1881 (s), 1864 (sh) cm^{-1} and 1920 (m), 1878 (s), 1802 (w) cm^{-1}, respectively. Crystals of **5** were identified from both single-crystal X-ray data and an IR spectrum, as previously described.[8h,i]

[14] In one of these reactions, different solvated crystals of **2** were isolated and identified from by X-ray crystallographic analysis. **2**·3 Me_2CO: triclinic; $P\bar{1}$; $a = 17.599(2)$, $b = 18.773(2)$, $c = 20.457(2)$ Å, $\alpha = 65.176(1)$, $\beta = 68.656(1)$, $\gamma = 66.086(1)°$, $V = 5452.4$ Å^3, $Z = 1$, $\rho_{calcd} = 2.648$ Mg m^{-3}. Compound **2**·3 Me_2CO has crystallographic $C_i(\bar{1})$ site symmetry. It is noteworthy that crystals of **2**·3 Me_2CO exploded in the absence of a solution environment, even in paratone(N) or epoxy components; they could only be stabilized for an X-ray diffraction study in a quickly hardening solution of polystyrene in Me_2CO/Et_2O.

[15] a) **1**·2 Me_2CO: monoclinic; $P2_1/n$; $a = 13.862(1)$, $b = 25.294(2)$, $c = 19.648(2)$ Å, $\beta = 97.882(1)°$, $V = 6824.2(9)$ Å^3; $Z = 2$, $\rho_{calcd} = 2.539$ Mg m^{-3}. $Mo_{K\alpha}$ data collected at 173(2) K with SMART CCD 1000 area detector diffractometer by 0.3ω scans over a 2θ range 3.2–56.6°; empirical absorption correction (SADABS) applied ($\mu(Mo_{K\alpha}) = 4.014$ mm^{-1}; max/min transmission, 0.856/0.379). Anisotropic refinement (695 parameters; 47 restraints) on 16927 independent reflections converged at $\omega R_2(F^2) = 0.126$ with $R_1(F) = 0.044$ for $I > 2\sigma(I)$; GOF (on F^2) = 0.92; max/min

  0044-8249/03/11503-0340 $ 20.00+.50/0

residual electron density, 2.19/−2.18 e Å^{-3}.Compound **1** has crystallographic $C_i(\bar{1})$ site symmetry such that the asymmetric part of the crystal structure consists of 1/2 of a neutral cluster and one solvated acetone molecule; b) **2**·2 Me_2CO: monoclinic; $P2_1/n$; $a = 17.517(1)$, $b = 24.471(2)$, $c = 24.216(2)$ Å, $\beta = 106.233(1)°$, $V = 9966.5(13)$ Å^3; $Z = 2$, $\rho_{calcd} = 2.878$ Mg m^{-3}. $Mo_{K\alpha}$ data collected at 173(2) K with SMART CCD 1000 area detector diffractometer by 0.3ω scans over 2θ range 2.9–56.6°; empirical absorption correction (SADABS) applied ($\mu(Mo_{K\alpha}) = 4.900$ mm^{-1}; max./min. transmission, 0.758/0.374). Anisotropic refinement (1044 parameters; 74 restraints) on 24577 independent reflections converged at $\omega R_2(F^2) = 0.158$ with $R_1(F) = 0.052$ for $I > 2\sigma(I)$; GOF (on F^2) = 0.99; max./min. residual electron density, 2.13/−2.56 e Å^{-3}. Compound **2** has crystallographic $C_i(\bar{1})$ site symmetry such that the asymmetric part of the crystal structure consists of 1/2 of a neutral molecule and one solvated acetone molecule. CCDC-195160 (**1**) and -195161 (**2**) contain the supplementary crystallographic data for this paper. These data can be obtained free of charge via www.ccdc.cam.ac.uk/conts/retrieving.html (or from the Cambridge Crystallographic Data Centre, 12, Union Road, Cambridge CB21EZ, UK; fax: (+44) 1223-336-033; or deposit@ccdc.cam.ac.uk).

[16] Observed electron counts of 372, 648, and 290 electrons were obtained for **1**, **2**, and **3**, respectively. Application of the Mingos electron-counting model[17] for a close-packed metal cluster gives rise to the following predicted electron counts: namely, 290 electrons (i.e., 12 × 18(surface) + 18(interior) + 4 × 14(wingtip)) for **3** and 378 electrons (i.e., 12 × 24(surface) + 34(two interior) + 4 × 14(wingtip)) for **1**. The highly condensed geometry of **2** prevents a reliable predicted electron count.

[17] a) D. M. P. Mingos, *J. Chem. Soc. Chem. Commun.* **1985**, 1352; b) D. M. P. Mingos, L. Zhenyang, *J. Chem. Soc. Dalton Trans.* **1988**, 1657.

[18] J. Donohue, *The Structures of the Elements*, Wiley, New York, **1974**, p. 216.

[19] In sharp contrast, corresponding mean radial Pd(i)–Pd(s_1) separations found in face-condensed icosahedral-based Pd-core geometries of high-nuclearity palladium carbonyl trimethylphosphine clusters are approximately 0.14 Å shorter than the mean tangential intrashell Pd(s_1)–Pd(s_1) separations (that is, 2.73 (av) versus 2.87 Å (av)).[9c] This large difference is ascribed to geometrically imposed radial compressions in icosahedral-based polyhedra. The close agreement of the mean Pd–Pd separations determined for the radial and tangential (intrashell) connectivities in **1**, **2**, and **3** point to the absence of geometrical distortions in the metal-core geometries of cuboctahedral-based systems.

Chemical Adaptor Systems

A Chemical Adaptor System Designed To Link a Tumor-Targeting Device with a Prodrug and an Enzymatic Trigger**

*Anna Gopin, Neta Pessah, Marina Shamis, Christoph Rader, and Doron Shabat**

Selective chemotherapy remains a key issue for successful treatment in cancer therapy. Prolonged administration of effective concentrations of chemotherapeutic agents is usually not possible because of dose-limiting systemic toxicities. Furthermore, strong side effects involving nonmalignant tissues are often observed. Therefore, much effort has been devoted to the development of new drug delivery systems that mediate drug release selectively at the tumor site. One way to achieve such selectivity is to activate a prodrug specifically by a confined enzymatic activity. In this concept, the enzyme is either expressed by the tumor cells, or brought to the tumor by a targeting moiety such as a monoclonal antibody.[1] The prodrug is converted to an active drug by the local or localized enzyme at the tumor site, thereby minimizing nonspecific toxicity to other tissues.

Here we present a new concept that combines a tumor-targeting device, a prodrug, and a prodrug activation trigger in a single entity. We designed a generic module or chemical adaptor that is based on three chemical functionalities as shown in Figure 1. The first functionality is attached to an active drug and**,** thereby, masks it to yield a prodrug. The second functionality is linked to a targeting moiety, which is responsible for guiding the prodrug to the tumor site, and the third functionality is attached to an enzyme substrate. When the corresponding enzyme cleaves the substrate, it triggers a spontaneous reaction that releases the active drug from the targeting moiety. As a result, prodrug activation will preferentially occur at the tumor site.

The central core of our chemical adaptor (Scheme 1) is based on 4-hydroxymandelic acid, which is commercially available and has three functional groups suitable for linkage. Group **I** is a carboxylic acid that is conjugated to a targeting moiety through an amide bond. The drug is linked through the benzyl alcohol group **II**, and the enzyme substrate is attached through the phenol group **III** by a carbamate bond.

[*] Dr. D. Shabat, A. Gopin, N. Pessah, M. Shamis, Dr. C. Rader
Department of Organic Chemistry
School of chemistry, Faculty of Exact Sciences
Tel Aviv University
Tel Aviv 69978 (Israel)
Fax: (+972) 3-640-9293
E-mail: chdoron@post.tau.ac.il

[**] We thank Professor Richard A. Lerner and Professor Carlos F. Barbas III of The Scripps Research Institute for providing antibody 38C2 and TEVA Pharmaceutical Industries Ltd., Israel for a gift of etoposide. We also thank Ms. Rajeswari Thayumanavan for early contributions to this work.

Supporting information for this article is available on the WWW under http://www.angewandte.org or from the author.